Arab J Geosci (2016) 9: 189
DOI 10.1007/s12517-015-2263-z

ORIGINAL PAPER

Flood hazard vulnerability for settlements of Turkey's province of Edirne, using ASTER DEM data and Landsat-7 ETM+ image data

Ali Can Demirkesen [1]

Received: 4 March 2015 / Accepted: 1 December 2015 / Published online: 10 March 2016

Abstract While Turkey's province of Edirne represents one of the country's most significant cultural heritage areas because it lies in the basins of the Meric and Ergene rivers, this very valuable region is highly susceptible to flooding during heavy rain falls. It becomes particularly vulnerable when neighboring Bulgaria responds to its own threats of heavy rain or snowfall by opening its floodgates of its dams on the River Meric, which flows through the Edirne province. Therefore, for years, the Edirne province has experienced severe floods that are eroding its fertile alluvial agricultural floodplains. An environmental plan based on a determination of the vulnerability levels of the province's flood hazard risk areas is required if action is taken to alleviate this problem. The objective of this study is to acquire geo-information from the remotely sensed data and to interpret the flood hazard risk levels of the area's settlements and agricultural floodplains. In this study, the spatial distribution of the flood hazard risk areas in the Edirne province is determined using not only the Advanced Space-Borne Thermal Emission and Reflection Radiometer digital elevation model data of the Edirne province to create maps that illustrate the digital terrain model and the 3D fly-through dynamic model of the study region but also the Landsat-7 Enhanced Thematic Mapper Plus multi-spectral image data set to create land use and land cover types of the study region. The maps exhibit landform characteristics, floodplain topography, and stream drainages. Analysis and interpretation of the maps demonstrate that the areas most susceptible to flooding are Enez, which lies at the northern coastal area of the Aegean Sea and agricultural areas, and the settlements on the Meric River floodplains of Ipsala, Meric, Edirne, and Uzunkopru, listed in decreasing order, respectively.

Keywords Flood hazard vulnerability · Remote sensing · Geographic Information System · Edirne, Turkey

✉ Ali Can Demirkesen
ademirkesen@yahoo.com

[1] Department of City and Regional Planning, Izmir Institute of Technology, Izmir, Turkey

Introduction

The Edirne province, one of Turkey's most significant cultural heritage sites, is located in a region of high-risk flooding in instances of heavy rainfalls and/or melting snow. Flood records in the Edirne province show that since 1940 the area has experienced 50 floods that resulted in loss of lives and property (MGM 2013). These disasters highlight the study region's high susceptibility to flooding. For years, the severe flooding in the Edirne province has been exacerbated by Bulgaria's opening of the floodgates of its dams on the River Meric, which flows through the Edirne province to the south before discharging its waters into the northern Aegean Sea. When the River Meric overflows its banks after heavy rain and/or melting snow, the resulting floods not only inundate social facilities, such as bridges, roads, streets, houses, workplaces, restaurants, cafes, and animal shelters located on near the river but also cause loss of lives. The first area subjected to the disastrous flooding is the administrative city of Edirne, located in the junction of the Meric, Arda, and Tunca rivers. The floods next affect the town of Ipsala and its low-lying agricultural floodplains located in the junction of the Meric and Ergene rivers. Finally, it affects Enez, before finally discharging into the northern Aegean Sea.

Many local governments have also been recently reporting that in times of heavy rainfall, the hazards of river floods have threatened those settlements built in low-lying agricultural

plain and/or valleys. This heavy rainfall and erosion is having an adverse impact on the economy and the country's ecosystems (Schanze et al. 2006).

One of the most important and commonly shared issues faced by policy makers is the management of flood disasters that have the potential of imposing both social and economic hardships. Therefore, policy makers need analysis tools and models to improve their decision-making processes so as to minimize the adverse effects of those flood disasters that are meteorology-based due to heavy rainfall caused by climate changes (Brivio et al. 2002; Schanze et al. 2006; Kim et al. 2011; Kandilioti and Makropoulos 2012).

While historical records of the Edirne province show that the region's population has always lived under considerable threat of flooding, a literature review reveals a paucity of analyses of the geological characteristics of the Edirne province in terms of its considerable flood hazard risk. Despite the lack of studies on Edirne per se, however, the literature does reveal a large number of research into similar concerns (Brivio et al. 2002; Wang et al. 2002; Van der Sande et al. 2003; Sanyal and Lu 2004; Schanze et al. 2006; Meyer et al. 2009). Some previous studies have investigated flood hazards similar to those discussed in our study. Among those are investigations of the effects of the Digital Terrain Model (DTM), landscape characteristics, and the topography-based watershed model. For example, Wang et al. (2002) used Landsat Thematic Mapper and Digital Elevation Model (DEM) data to map the extent of flooding in coastal flood plains. These authors described an efficient and reliable method for mapping flood areas in coastal flood plains and modeling inundation using the DEM data. Van der Sande et al. (2003) looked at flood risk and flood damage assessment. They created land cover maps from high-resolution satellite imagery, the Ikonos, to assist the flood risk and flood damage assessment. Sanyal and Lu (2004) and Schanze et al. (2006) studied the hazards, vulnerability, and mitigation measures for flood risk management. Brivio et al. (2002), Meyer et al. (2009), Ho et al. (2010), Hoque et al. (2011), and Kandilioti and Makropoulos (2012) studied flood monitoring and mapping using remote sensing (RS) integrated with Geographic Information System (GIS).

The objectives of this study are to both acquire geo-information about the Edirne province of Turkey using the remotely sensed data and to describe the flood hazard risk levels to settlements and agricultural areas in the study region. The main data sources are the Advanced Space-Borne Thermal Emission and Reflection Radiometer (ASTER) DEM data and the Landsat-7 ETM+ multi-spectral image data set of the study region. Existing landscape characteristics are also analyzed for the flood hazard vulnerability. By quantifying and analyzing the DTM (Wilson and Gallant 2000) and hydrological features of the Edirne province, geo-information is acquired to help (1) control and extend the existing flood hazard precaution and prevention measures, (2) evaluate the suitability and flexibility of current regional development plan strategies in relation to the flood hazards, and (3) assist in decision-making regarding future land planning and efficient flood management in the study area. In this study, the major river drainages and water flow accumulation areas that indicate flood-prone zones are also investigated and analyzed in terms of flood hazards.

Our results/findings and the maps created in this study significantly contribute to environmental planning in the Edirne province, where the river flood hazards are important concern. This study also demonstrates the analysis of digital terrain, elevation classification, extraction of river drainages, and describing water accumulation areas with land use/land cover types using the RS integrated with the GIS.

Developing high technologies in the RS and GIS have eased data collection and processes for the flood hazard risk interpretation of the settlements. By employing the RS techniques integrated with the GIS, we not only analyze the DTM and the landscape characteristics but also extract and analyze the stream drainages in terms of the flood hazard.

Thus, the objectives of this study are the following: (1) firstly, to obtain geo-information about the study region by generating the DTM, exhibiting the landforms, floodplain topography, and watersheds; (2) secondly, to determine spatial distributions of the settlements having the river flood hazard risks overlaid with the land use/land cover (LULC) types; and (3) finally, to contribute to decision-making on any future environmental planning, efficient flood management, and to preserve settlements and ecosystems.

Study region

The Edirne province is roughly located at 26°–28° E meridians and 40°–42° N parallels (Fig. 1). While the total study region is 21,260 km^2, according to 2011 statistics (TUIK 2013), the province of Edirne has an area of 6276 km^2 and a population of about 400,000. The Edirne province is surrounded by the provinces of Kirklareli and Tekirdag to the west, the country of Bulgaria to the north, Greece to the east, and the Aegean Sea to the south.

The study region has Mediterranean and Marmara climates with a mild winter and mean annual precipitation of about 850 mm and a hot summer. The heavy rainfall it generally receives in spring is the cause of its floods. Its average temperature is 5 °C in January and 25 °C in July (Atalay 2008; Edirne Governorship 2013; MGM 2013).

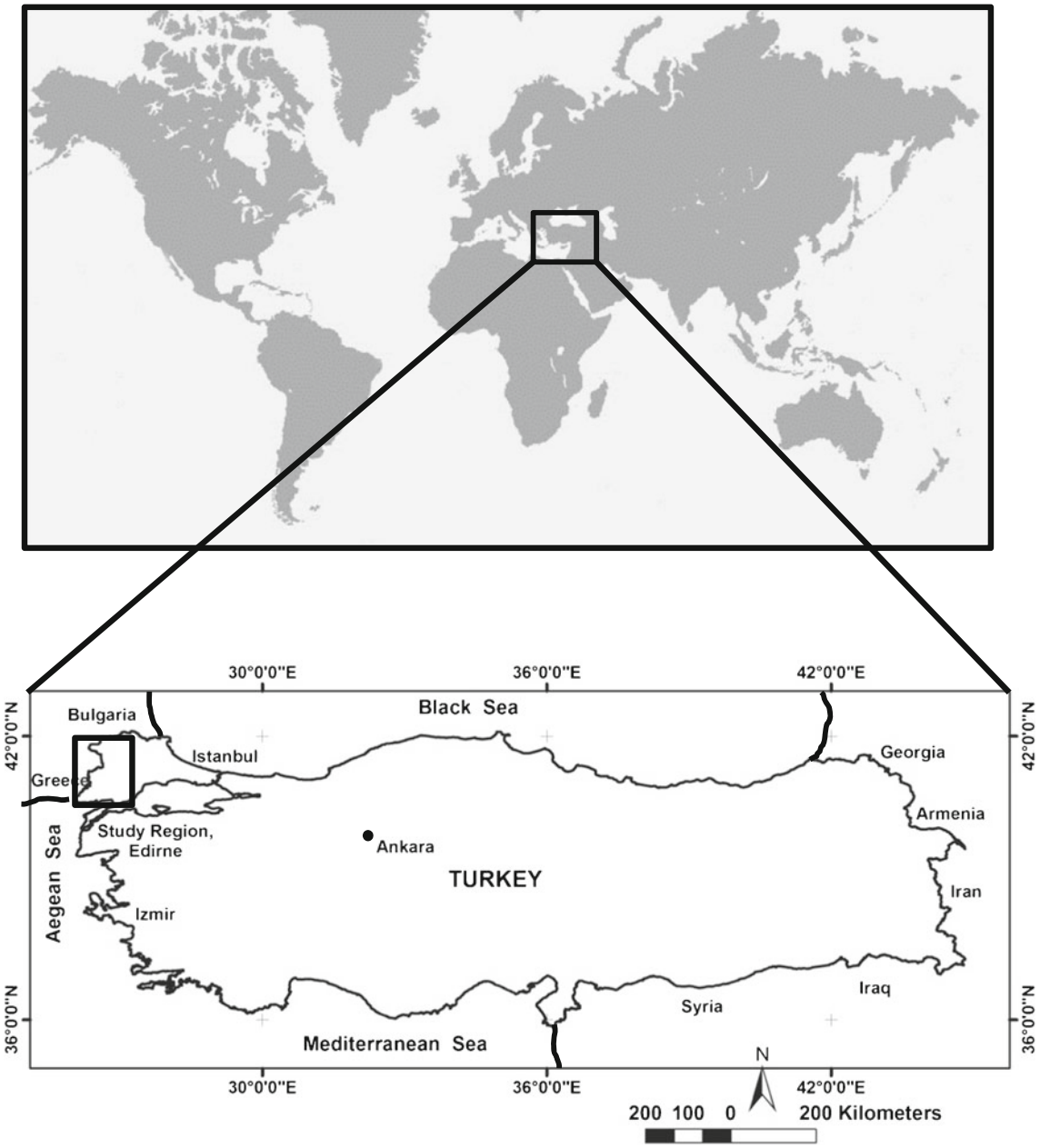

Fig. 1 Location of the Edirne province

The Edirne province is located in the greater region of Eastern Thrace (termed *Trakya* in Turkish) along the borders of Greece and Bulgaria. The Edirne province has nine administrative areas: the provincial seat of Edirne and the counties of Enez, Havsa, Ipsala, Kesan, Lalapasa, Meric, Suloglu, and Uzunkopru. The provincial seat of Edirne is a gateway city, connecting Turkey to Europe. It is settled on slopes and the fertile river flood plains formed by the junction of the three rivers: Meric, Tunca, and Arda. The River Meric (Maritza) originates in Bulgaria and flows through the border between the province of Edirne and Greece. The river discharges into the northern Aegean Sea at Enez. The Tunca and Arda rivers, both sub-tributaries of the River Meric, flow from Bulgaria and meet the River Meric at the city of Edirne. The Edirne province also has a second major river called the Ergene which flows from Kirklareli before merging with the River Meric at Ipsala and then flowing to the Aegean Sea through Enez. The Meric and Ergene rivers merge in the Ergene basin, a water accumulation area that faces the threat of flood hazards. While the region does have a few hills and slopes, the province of Edirne does not have any high mountains within its borders and none of its hills surpasses 500 m in height. Most of the province consists of flat agricultural plains. The province is also largely deforested (Atalay 2008; Baykan 2004; GEODATA 2013).

Data

ASTER DEM data

The ASTER DEM data were gained by means of an international joint project undertaken between the Ministry of Economy, Trade and Industry of Japan (METI) and the National Aeronautics and Space Administration (NASA). The ASTER, which is a space-borne earth-observing optical instrument, consists of an earth-observing sensor developed in Japan that is onboard the satellite *Terra*. Since its launch in December 1999, the sensor has continued to operate for more than 10 years in a stable manner. The sensor comprehensively captures spectral ranging from visible to thermal infrared (invisible to the human eye) and offers detailed information on earth surface conditions (e.g., vegetation, geological features) together with their distribution. The distribution of surface temperature can be observed by the thermal infrared sensor. These data support detailed studies of such phenomenon as the urban heat island effect. The ASTER elevation data are generated from a stereo-pair of images acquired with nadir and backward angles over the same area (ASTER GDEM 2013; ERSDAC 2013).

The ASTER elevation data in the geographic coordinate system, WGS84 datum, were obtained from the Consortium for Spatial Information, in the format of Geotiff as 32 bits. The ASTER mainly operates in the microwave wavelengths of electromagnetic spectrum and uses radar sensors for the collection of DEM data. The ASTER elevation data have the spatial resolution of 30 m, with horizontal and vertical accuracies of 15 and 8 m, respectively (San and Suzen 2005; ASTER GDEM 2013; ERSDAC 2013).

Landsat-7 ETM+ multi-spectral image data

Geometrically and radiometrically rectified Landsat-7 Enhanced Thematic Mapper Plus (ETM+) multi-spectral image data set of the study region was used for classification of LULC types. The Landsat-7 ETM+ image set dated 2 July 2000 and in geographic coordinates was obtained from the Global Land Cover Facility (GLCF), Earth Science Data Interface (ESDI) (GLCF 2013). The Landsat-7 ETM+ is a multi-spectral scanning radiometer carried onboard the Landsat satellite that provides a multi-spectral image data set from eight spectral bands. The spatial resolution is 30 m for the visible and near-infrared (bands 1–5 and 7). Resolution for the panchromatic (band 8) is 15 m, and the thermal infrared (band 6) is 60 m (GLCF 2013).

Maps and GIS layers

Digital topographic and LULC map layers of the study region at the scale of 1:100,000 were obtained from the General Command of Mapping (Turkish: Harita Genel Komutanliği, HGK) (HGK 2013). These digital maps include a few numbers of the GIS layers. Such layers are settlements, settlement centers, forests, housings, rivers, lakes, roads, and boundary maps of the study region. These GIS layers as quadrangles were generated from the base maps of the standard topographic quadrangles at the scale of 1:100,000 which were originally produced by the HGK (HGK 2013). All these maps and GIS layers were used for geo-referencing as well as overlaying and comparing with the other resultant maps from the ASTER elevation data and the Lansat-7 ETM+ imagery.

Higher-resolution ground data

Two hundred ground control points (GCPs) as reference points were collected by the field work activities using a hand-held GPS with horizontal coordinates and attributes with spatial horizontal expected error of ±3 m in addition to both higher-resolution images of the Google Earth and the topographic maps (HGK 2013). These data were used for geo-referencing and ground truth, as well as for accuracy assessment of the image classification (Congalton 1991; Congalton and Green 1999; Lillesand and Kiefer 2004; Jensen 2005). Most of the GCPs were visible on the higher-resolution imagery, such as intersections of the major rivers, roads, and sharp corners of buildings as well as distinctive points.

Method

Processing the ASTER DEM data

A methodology to process multi-scaled different data sources as spatial data (coordinate information) in addition to non-spatial data (attribute information) of the study region was created for the flood hazard risk interpretation (Fig. 2). The methodology used to analyze the digital terrain (Wilson and Gallant 2000; El Sheimy et al. 2005) of the study region is depicted in Fig. 2. To pre-process the data, the Landsat-7 ETM+ multi-spectral image data set and the ASTER elevation data were co-registered using the reference system for satellite imagery in GeoTIF format with grid size 30 m, the WGS84 datum, and the UTM projection coordinate system with zone number 35N. Then, the entire study region was extracted using *Extract by Mask* tool of the Extraction Menu in the ArcGIS system (ArcGIS 2013) and imported to the Idrisi Selva system (IDRISI 2013) for later processes, such as classification and analysis of the elevation and image data.

The ASTER DEM with spatial resolution of 30 m in geographic coordinates (λ, φ degrees) obtained from the Internet

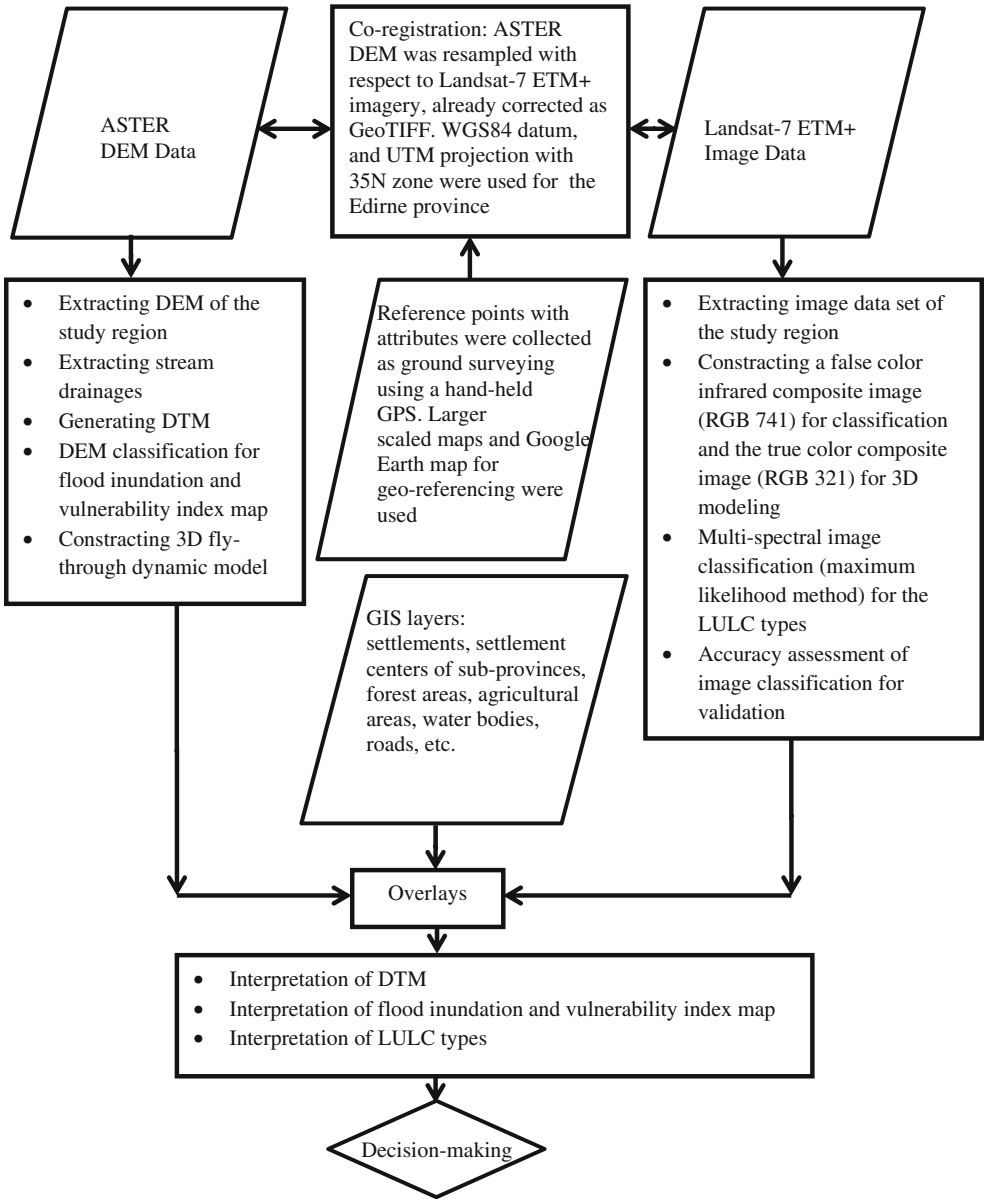

Fig. 2 Methodology: steps of the data processes involved in the flood hazard vulnerability for settlements of the Edirne province

(ASTER GDEM 2013; ERSDAC 2013) was used to classify the elevation data and to extract the stream drainage patterns in the study region.

Before classification, using the *Projection* tool in the ArcGIS system (ArcGIS 2013), the elevation data were automatically transformed from geographic coordinates (λ, φ degrees) into the UTM projection system coordinates (*x*, *y* meters) with zone number 35N and the WGS84 datum. Next, using the *Extract by Mask* tool of the extraction menu in the ArcGIS system (ArcGIS 2013), the relevant elevation data were extracted according to the boundary of the Edirne province. After that, the extracted elevation data were entered into the Idrisi Selva system for other processing such as the 3D fly-through dynamic image generation. However, the data processes were done using both the ArcGIS and Idrisi systems.

Landforms and stream drainages, coastal flood plains, agricultural plains, plateaus, and mountain areas in the study region were determined from the classification of the ASTER elevation data. Next, the landforms and risk areas were described according to the properties of the stream drainages, and water accumulation areas and were analyzed using the GIS.

The ASTER elevation data were used for extraction of the stream drainages and then were used for analyzing the landforms. Shaded DEM was used to characterize the DTM (Fig. 3) to extract geo-information such as slopes and aspects. For the flood risk interpretation, several operations on the elevation data were performed through the ArcGIS (ArcGIS 2013). First, the DTM, a 24-bit color image of the shaded DEM data (Fig. 3), was generated and analyzed by overlaying

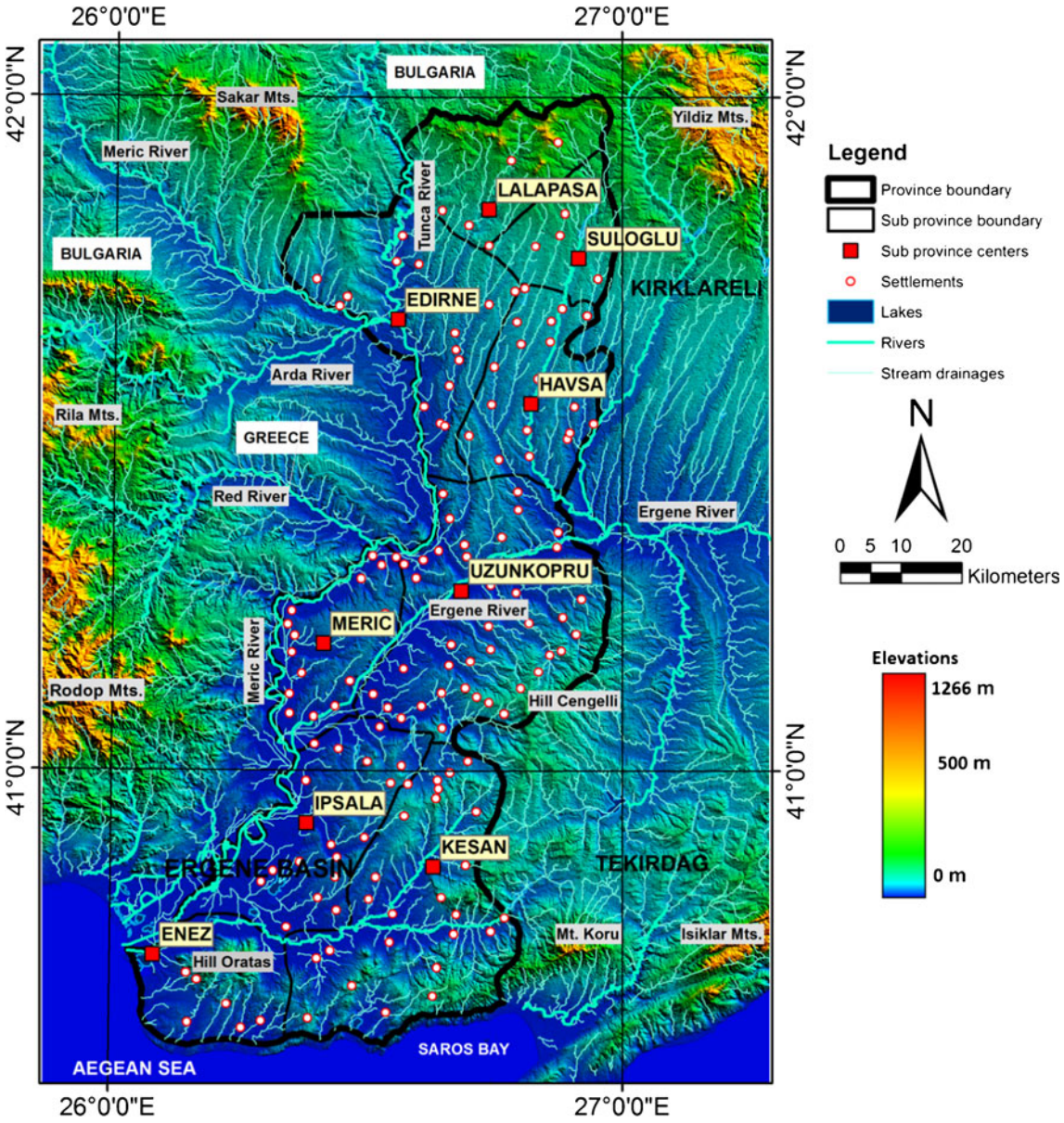

Fig. 3 Digital Terrain Model (DTM) of the Edirne province produced from the ASTER DEM data via the ArcGIS system

settlements, main stream drainages, and their sub-tributaries. Then, the elevation data were classified to identify the main landforms such as valleys, plains, plateaus, hills, and mountains (Fig. 4 and Table 1). The elevation data was also used to generate a perspective view of the 3D fly-through dynamic model via the Idrisi Selva system.

The raster cells with the elevations (1) from 0 to 5 m were designated as coastal flood risk areas (very high vulnerable areas I); (2) 5 to 10 m river flood plains I (very highly vulnerable areas II); (3) 10 to 25 m river flood plains II (highly vulnerable areas); (4) 25 to 50 m river flood plains III (medium vulnerable areas); (5) 50 to 200 m plain areas (low vulnerable areas); (6) 200 to 500 m mountain areas; and (7) 500 to 1266 m high mountain areas (Table 1) after interactively analyzing the displayed elevation data by the tool of *Display Min/Max Contrast Setting* in the Idrisi Selva system. For the elevation data classification, sudden and abrupt slope changes in the terrain were considered by interactive analysis. For instance, elevations of locations, where agricultural flat plains finish and mountains slopes start, were considered for classification intervals and/or thresholds. Besides, water flow inflation points (merging river flows), water flow direction (from upper elevation to lower elevation), water flow accumulation areas (valleys and flat plains), slopes, and aspects were considered for vulnerability index analysis.

For the elevation classification, the elevation intervals were subjectively determined (user-determined thresholds)

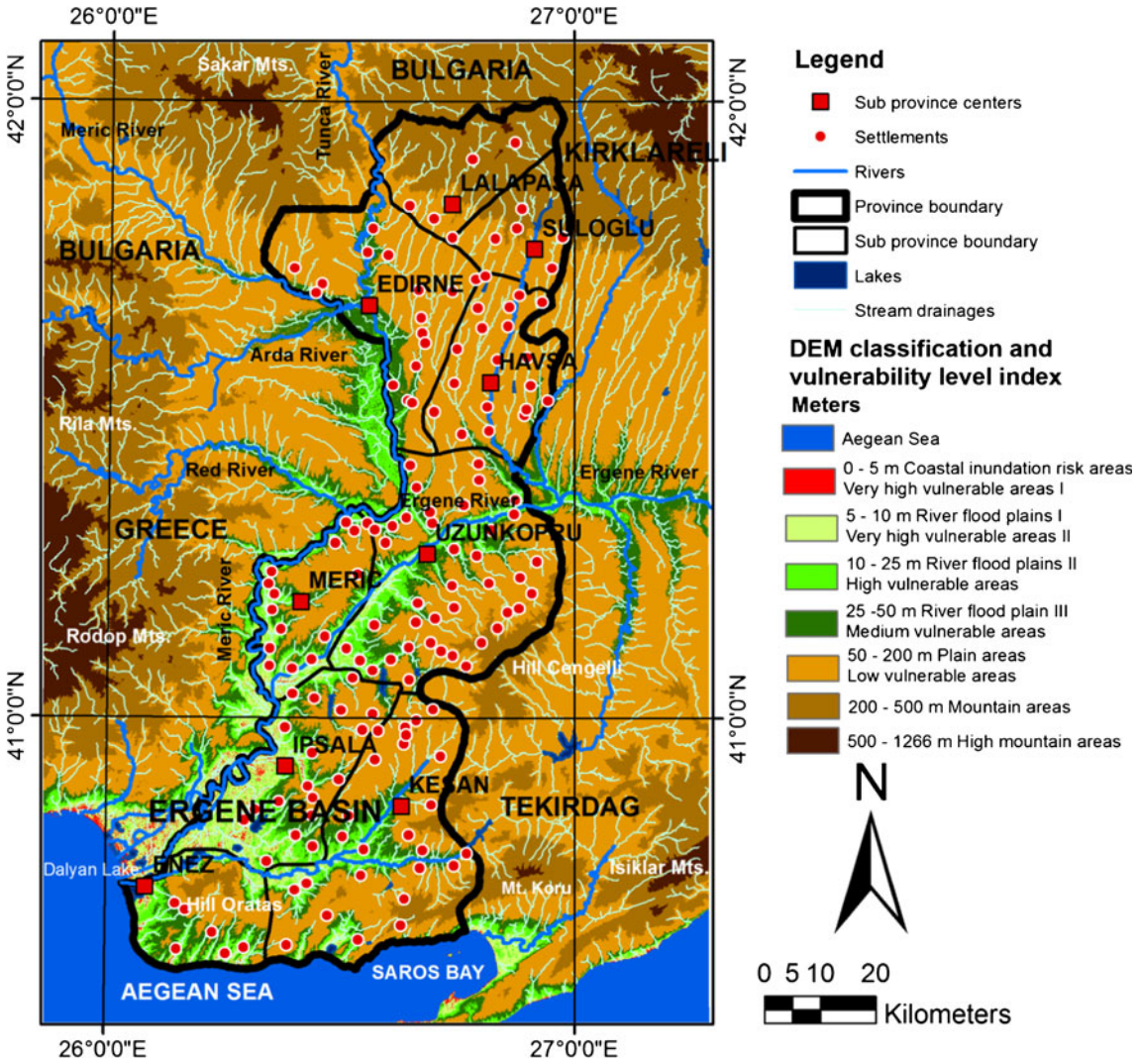

Fig. 4 The flood inundation and flood hazard vulnerability index map of the Edirne province produced from the ASTER DEM classification via the ArcGIS system

using the DEM visualization function in the ArcGIS system. These elevation classification intervals correspond to sudden color changes, slopes, and aspects, which indicate a sudden change in the terrain surface, representing the borders of the valleys, flat plains, plateaus, hills, and mountains. Therefore, the classified elevation levels and the number of intervals used in the analysis can vary depending on the user-defined thresholds. The elevation intervals were determined by examining the topographic characteristics of the surface of the study area.

After the DEM classification of the landforms and analysis, maps of the mainstream drainage hierarchy, i.e., the *Strahler* stream orders, were generated from the ASTER elevation data via the *Hydrology* tool in the ArcGIS system (Mark et al. 1984; O'Callaghan and Mark 1984; Band 1986; Ozdemir and Bird 2009).

For the river flood risk interpretation, the outputs of the hydrological data processing, i.e., the DTM, the elevation classification, and the perspective view of the 3D fly-through dynamic model which indicates landforms, channels of major rivers, hierarchical stream drainages, pour points (junctions of major rivers), and water flow accumulation areas were overlaid with the settlements, roads, rivers, and lakes of the Edirne province.

In the flooding risk interpretation process, five criteria were considered to determine the risk levels for the settlements under threat of flooding: (1) the *Strahler* stream orders, hierarchies of water-flow inflection of the major river channels via Hydrology tool in the ArcGIS system (ArcGIS 2013); (2) distance from the settlements to the overflow zones of the major river channels; (3) distance from settlements to the major river channels; (4) slopes and aspects of the settlement areas, i.e., flat agricultural plains and valleys; and (5) distance from settlements to water flow accumulation areas and pour points where rivers merge.

Table 1 Results of the ASTER DEM classification for river flood hazard vulnerability of the Edirne province

DEM classification		Area (km^2)	Total (%)	Dominant land cover types
0–5 m	Coastal inundation risk areas	18	0.01	Agriculture/water body/settlement
5–10 m	Very highly vulnerable areas I River flood plains I	930	15.0	Agriculture/water body/settlement
10–25 m	Very highly vulnerable areas II River flood plains II	750	12.0	Agriculture/settlement/water body
25–50 m	Highly vulnerable areas River flood plains III	500	8.0	Agriculture/settlement/forest/water body
50–200 m	Medium vulnerable areas Plain areas	3138	50.0	Agriculture/settlement/forest/water body
200–500 m	Low vulnerable areas Mountain areas	940	15.0	Forest/bare rock
500–1266 m	High mountain areas	0	0.0	Forest/bare rock
Total area of Edirne province		6276	100.0	

Grid size resolution = 30 m; horizontal accuracy = 15 m; vertical accuracy = 8 m. The total area of the whole study region including outside of the Edirne province is 21,260 km^2 . Elevations of 500–1266 m indicating high mountains in the whole study area are 14,984 km^2

Processing the Landsat-7 ETM+ multi-spectral image data

The Landsat-7 ETM+ multi-spectral image data set of the study region, corrected and registered as GeoTIFF, with 30 m resolution, was obtained from the Global Land Cover Facility (GLCF 2013). After having the image data set in the UTM projection coordinate system with zone number 35N and the WGS84 datum, the relevant parts were extracted using the *Mask* operation according to the boundary layer of the study region in the UTM projection coordinate system of the Edirne province obtained from the General Command of Mapping (HGK 2013). The extracted image data set was then imported to the Idrisi Selva system (IDRISI 2013) using the maximum likelihood classification (MLC) for the LULC types (Lillesand and Kiefer 2004; Jensen 2005).

Using the *Composite* tool, the infrared false color composite image RGB 741 was generated by assigning the seventh band of the Landsat-7 ETM+ image data set to the red (R) channel, the fourth band as an infrared band to the green (G) channel, and the third band to the blue (B) channel in the Idrisi Selva system (IDRISI 2013). The RGB 741 image was used to define the *training data* set for the MLC. Similarly, the true color composite image RGB 321 was also generated to construct the fly-through dynamic model.

The MLC is a *classifier* that quantitatively determines both the variance and the covariance of the classes of the pixels in the image bands when grouping the pixels. In this method, an assumption is made such that the pixels in the training classes in the spectral bands are normally distributed. Therefore, the distributions of the classes (grouped pixels of land cover types) can be completely described by the mean vector and the covariance matrix. With these parameters, we can determine the statistical probability of a given pixel value being a member of a specific land cover class (Lillesand and Kiefer 2004; Jensen 2005).

In the Idrisi Selva system, the *Maxlike* (maximum likelihood classifier) tool was used to execute the MLC of the Landsat-7 ETM+ image data set for the LULC classification based on the information in the set of signature files, generated by the *Makesig* tool from the training data set, which was defined by on-screen digitizing on the false color composite image RGB 741. The MLC uses the probability density function corresponding to a specific training class signature of the land cover. Pixels are assigned to the most likely class based on a comparison of the posterior probability that it belongs to each of the signatures being considered (IDRISI 2013).

To detect the LULC types (Fig. 5) in this study, the Landsat-7 ETM+ image set of 21,260 km^2 including outside of the Edirne province was classified using the MLC method in the Idrisi Selva system (IDRISI 2013). The supervised MLC was performed initially with 12 subclasses using 12 training data set of the land cover. The resultant 12 sub-classes were merged into five classes: settlement, agricultural plain, forest, water bodies, and bare ground (Fig. 5 and Table 2). Therefore, determination and analysis of the LULC from the satellite image set were carried out based on the MLC method. To determine the accuracy of the image classification for validation, a stratified random sampling method were used, making use of the 200 ground control points, collected by the field work activities using a hand-held GPS, with their

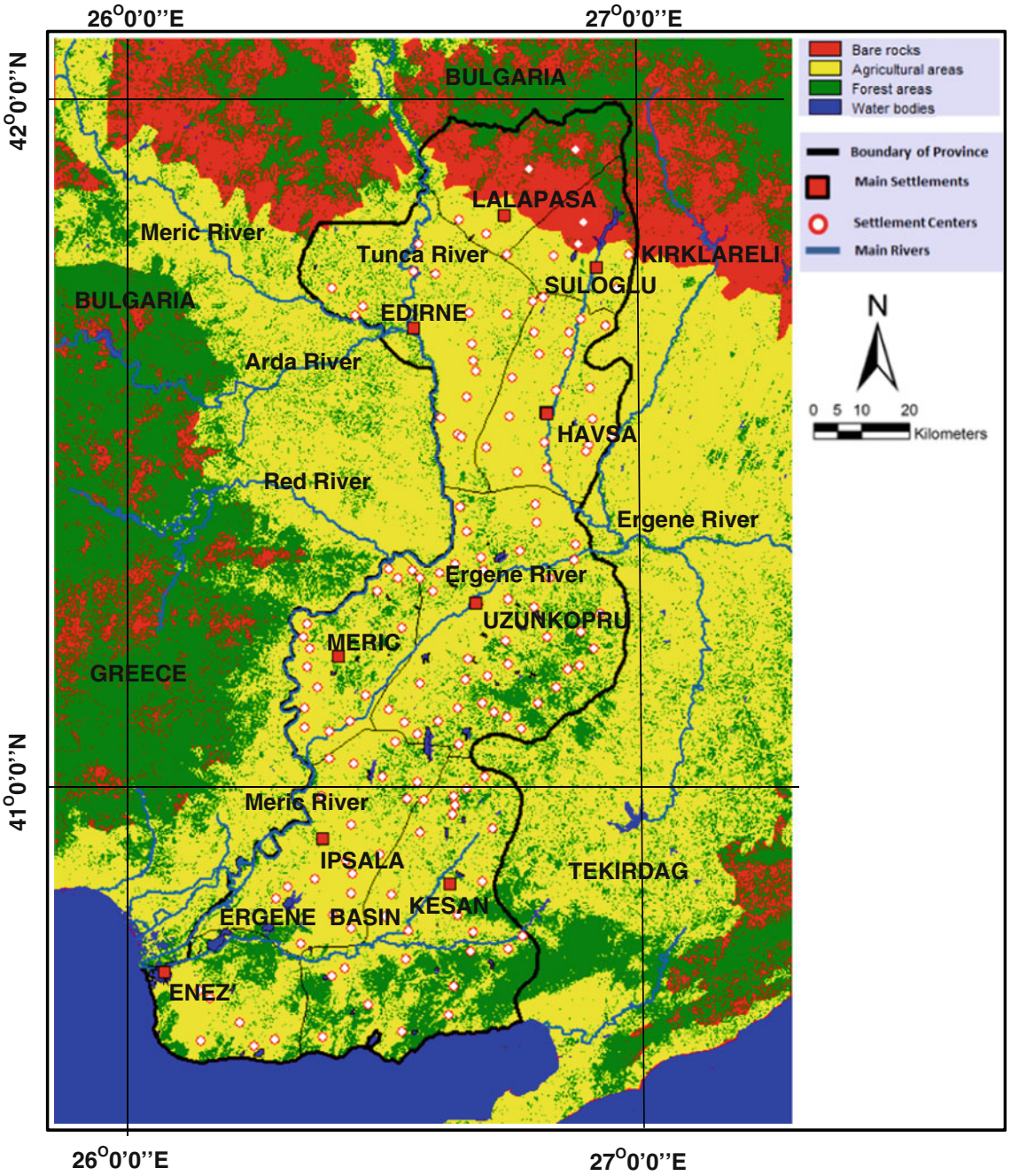

Fig. 5 Land use/land cover (LULC) types of the Edirne province produced from the maximum likelihood classification of the Landsat-7 ETM+ imagery via the Idrisi Selva system

attributes for the classified image (Congalton 1991; Congalton and Green 1999; Lillesand and Kiefer 2004; Jensen 2005; IDRISI 2013).

In terms of the delineation of the river flood risk areas with their LULC types, the procedure of the flood risk interpretation was depicted in Fig. 2. The Landsat-7 ETM+ imagery of the Edirne province was first classified to detect the LULC types. Second, areas most vulnerable to the flood in the study region were determined using the ASTER elevation data classification. The LULC types were determined by using the MLC method (Lillesand and Kiefer 2004; Jensen 2005; IDRISI 2013). Next, the results of both the image and elevation data classifications were overlaid to interpret the river flood risk areas, river flood plains of Ergene and Meric rivers in our case, with the LULC types. Finally, the flood hazard risk areas were computed, analyzed, and interpreted using both the ArcGIS and the Idrisi Selva systems.

Table 2 Results of the Landsat-7 ETM+ multi-spectral image classification for LULC of the Edirne province

LULC classification	PA (%)	UA (%)	Kappa	Area (km^2)	Total (%)
Agricultural areas	85	85	85	3766	60
Forest areas	95	95	95	1569	25
Settlements	85	85	85	125	2
Water bodies (lakes/rivers)	98	98	98	188	3
Bare rocks	85	85	85	628	10
Total area of the Edirne province				6276	100

Landsat-7 ETM+ imagery of July 2000, grid size of 30 m, and horizontal accuracy of 15 m. The total study area including outside of the Edirne province is 21,260 km^2

PA producer's accuracy, *UA* user's accuracy

Results and discussion

The novelty of this study is that the methodology in Fig. 2 uses integration of remote sensing and geographical information system technologies for decision-making where data come from different sources, types (raster and vector), multi-scales, and accuracies as a data fusion. In addition, quantitative and visual 3D analyses and interpretation were accomplished for decision-making in terms of flood hazard vulnerability. For interpretation, geomorphological landforms and floodplain topography, in particular, stream drainages and water accumulation areas were overlaid with spatial distribution of settlements in 3D.

In the study, the methodology was used to identify the susceptibility of the settlements and agricultural areas to the river flood hazard. First of all, the DTM in Fig. 3 was generated. Secondly, the flood inundation and flood hazard vulnerability index map in Fig. 4 was generated from the ASTER elevation data classification. Based on the ASTER DEM classification, the findings revealed that (1) coastal flood risk areas with elevations of 0–5 m as very highly vulnerable areas are 0.01 % of the Edirne province (6276 km^2); (2) flood plains I with elevations of 5–10 m, once again, as very highly vulnerable areas cover 15 %; (3) river flood plains II with elevations of 10–25 m as highly vulnerable areas cover 12 %; (4) 25 to 50 m river flood plains III as medium vulnerable areas are 8 %; (5) 50 to 200 m plain areas as low vulnerable areas are 50 %; and (6) 200 to 500 m mountain areas are 15 %. There is no high mountain area within the Edirne province (Fig. 4 and Table 1).

Thirdly, the Landsat-7 ETM+ multi-spectral image classification in Fig. 5 was generated. Based on the Landsat-7 ETM+ multi-spectral image classification, the findings revealed that (1) agricultural plain areas are 60 % of the study region (6276 km^2); (2) forest areas cover 25 %; (3) the settlement areas cover 2 %; and (4) water bodies (lakes, dams, and rivers) cover 3 % of the Edirne province (Fig. 5 and Table 2). Fourthly, the fly-through dynamic model in Fig. 6a was generated by draping the true color composite image, RGB 321, onto the ASTER elevation data via the *Fly-through* tool in Idrisi Selva system. Figure 6b was generated by draping the DTM image onto the ASTER DEM elevation data. The overlay of the DEM with the LULC types revealed that all of the flood risk areas are dominantly covered with the agricultural plain areas. Mountain areas are mostly covered with forests. The results are also compared and interpreted with higher-resolution satellite images (Fig. 7) coming from the Google Earth.

The DTM, flood inundation map, fly-through dynamic model, and LULC types as well as enlarged high-resolution satellite images of the study region from the Google Earth (Figs. 3, 4, 5, 6, and 7) indicate that the Meric and Ergene river flood plain areas and the settlements of all over Enez, western Ipsala, western Meric, southwestern Edirne, and northwestern Uzunkopru with their surrounding agricultural plains in decreasing order, respectively, are under threat of flood hazards. From the result, in general, we may say that the most risky areas are the locations where the main subtributaries merge and exacerbate severe flooding. In this study, that part of Edirne where the River Meric merges with its subtributaries, Arda and Tunca, represent the area with the highest risk. The study indicates that the highest flood risk areas are the agricultural areas that lie in the river flood plains of the Meric and Ergene rivers in the Ergene Basin (Figs. 3, 4, 5, 6, and 7, Table 3).

The elevation classification (Fig. 4) shows that the majority of settlements in Edirne province are located in low-lying agricultural areas with elevations ranging between 50 and 200 m. The river flood plains are primarily located in valleys, particularly the major river channels of the rivers of Meric and Ergene in the Basin Ergene with elevations of 0–50 m. From the results, the flood hazard vulnerability starts with elevation of about 50 m from the sea level in this study case, and we may say that the flood hazard vulnerability increases as elevations above the sea level are decreasing.

The accuracy of the DEM data depends on the resolution of the grid size, sampling errors and quality of measurements, co-registration, and interpolation techniques. The use of higher-resolution DEMs such as LiDAR and imageries such as GeoEye could produce more accurate and detailed results.

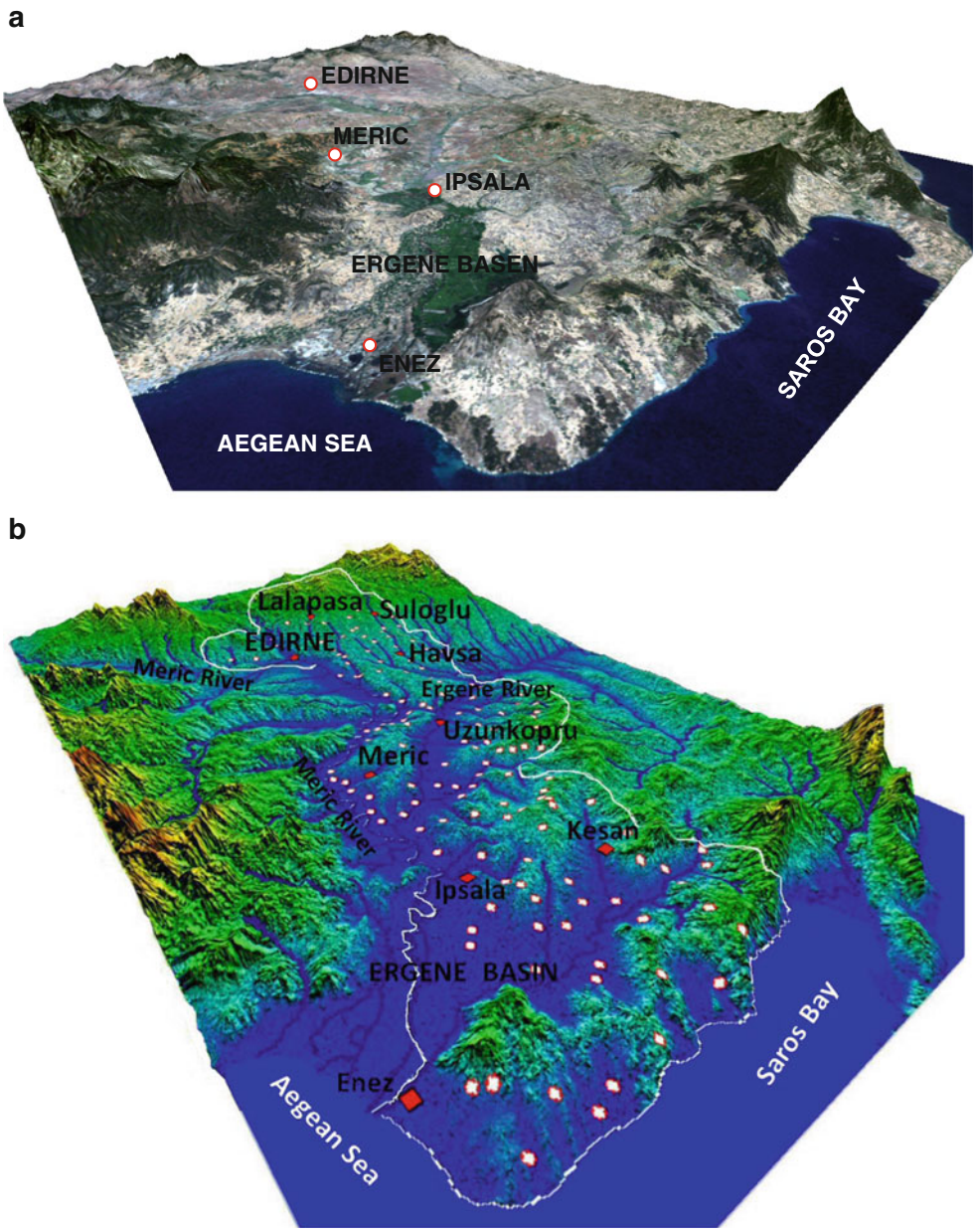

Fig. 6 **a** A perspective view of the 3D fly-through dynamic model of the Edirne province showing flood vulnerability areas. This image was created from the true color composite image (RGB = 321) of the Lansat-7 ETM+ multi-spectral image data set draped on the ASTER DEM data via the Idrisi Selva system. **b** A perspective view of the 3D fly-through dynamic model of the Edirne province showing flood hazard vulnerability areas, landforms, floodplain topography, main river channels, and water accumulation areas overlaid with settlements. This image was created by draping the DTM image onto the ASTER DEM data via the Idrisi Selva system

All the results coming from the ASTER elevation data and the Landsat-7 ETM+ multi-spectral image data with other topographic and thematic maps having the different accuracies and scales mentioned above, revealed the Figs. 3, 4, 5, 6, and 7 and Tables 1, 2, and 3 with these accuracies, the risky flood agricultural plains, and the settlements in the study region were interpreted and presented after quantitative and visual analyses.

In the accuracy assessment for this study, first of all, the ASTER elevation data have the spatial resolution of 30 m, with horizontal and vertical accuracies of 15 and 8 m, respectively (San and Suzen 2005; ASTER GDEM 2013; ERSDAC 2013), and the Landsat-7 ETM+ multi-spectral satellite image set have 30 m spatial resolution, so horizontal accuracy of 15 m (GLCF 2013), were used in this study. Secondly, 200 reference points as ground control points, also visible on the Landsat-7 ETM+ satellite images by the field work activities using a hand-held GPS with spatial horizontal expected error of ±3 m, were collected and used in the stratified random sampling for the ground truth for the accuracy assessment of the image classification validation (Congalton 1991; Congalton and Green 1999). Finally, the resulting overall classification accuracy of the Landsat-7 ETM+ multi-spectral imagery was 88 %, with Kappa values of 0.88 (Table 2). For more detailed information about accuracy assessment of multi-spectral image classifications, see the Classification

Fig 7 Enlarged satellite images of the river flood hazard risk areas from the Google Earth. These images illustrate the flood hazard risk areas of agricultural floodplains and settlements in the Edirne province affected by the rivers of Meric and Ergene. Source of the satellite images: Google Earth

Accuracy chapter in Lillesand and Kiefer (2004). Classification of water bodies and forests were more accurate than that of the settlements and agricultural land. Overall accuracies, producer's and user's accuracies, and *Kappa* values for the LULC types were derived from the error matrix. The error matrix includes the columns total, rows total, number of correctly classified cells (diagonal cells), errors of omission (exclusion) and commission (inclusion), an overall accuracy, confidence intervals, and the *Kappa* statistic for all classes on a per category basis. The overall accuracy of the classification

Table 3 Results of flood hazard vulnerability for settlements of the Edirne province

Settlements of sub-provinces under flood hazard vulnerability		Population of settlements (year 2011)	Main water bodies	Main river flood plains	Mounts or hills (meters)
Edirne		162,200	Meric river located in Edirne, Meric, Ipsala, and Enez, i.e., border between the Edirne province and the Greece country Tunca river in Edirne Ergene river in Uzunkopru and Ipsala	Meric flood plain in Edirne, Meric, Ipsala, and Enez Tunca flood plain in Edirne Ergene flood plain in Uzunkopru and Ipsala Havsa flood plain in Havsa and Suloglu Suloglu flood plain in Suloglu	Hisardag (423) in Enez Buyuktavsantepe (456) in Lalapasa Suleymaniyedag (378) in Uzunkopru Hidirelleztepe (371) in Kesan Karahöyüktepe (269) in Uzunkopru Yilanlitepe (239) in Edirne
	Kapikule	–			
	Karakasim	580			
	Elcili	405			
	Doyran	760			
	Uyuklutatar	730			
	Avariz	305			
	Degirmenyani	450			
	Yolustu	290			
	Suakacagi	100			
	Sazlidere	540			
Kesan		79,700	Havsa creek in Havsa and Suloglu Suloglu creek in Suloglu Ova creek in Uzunkopru	Ova in Uzunkopru Kocacay in Uzunkopru Dogancacay in Kesan	Ortatastepe (113) in Kesan Karatepe (109) in Meric Bagtepe (365) in Suloglu
	Sigilli	770			
	Kilickoy	550			
	Karahisar	280			
	Akhoca	515			
	Orhaniye	395			
Uzunkopru		66,100	Kocacay creek in Uzunkopru Dogancacay creek in Kesan Dalyan lake in Enez Gala lake in Enez Tasalti lake in Enez Celtik lake in Enez		Bagtepe (365) in Suloglu Candirtepe (385) in Enez Korudag (675) in Tekirdag Muhiddinbabatepe (600) in Lalapasa Istranca (Yildiz) mountains (590) in Suloglu, Lalapasa and Kirklareli
	Derekoy	815			
	Sazlimalkoc	395			
	Ciftlikkoy	190			
	Sigircili	295			
	Kiremitcisalih	470			
	Eskikoy	500			
	Saclimuselim	100			
	Gemici	220			
	Altinyazi	425			
	Muhacirkadi	305			
	Balabankoru	425			
Havsa		20,500			
Ipsala		29,800	Golbaba lake in Edirne central city Akcadam dam lake in Meric Pamuklu lake in Ipsala Sigircik lake in Ipsala		
	Karaagac	250			
	Yenikarpuzlu	3150			
	Pasakoy	1150			
	Ahir	305			
	Sarpdere	510			
	Turpcular	650			
	Saricaali	745			
	Balabancik	530			
	Tevfikiye	220	Sultanhankoy dam lake in Ipsala		
	Ibriktepe	1490			
	Lake Pamuklu	–			
	Lake Sigirci	–	Tuzla lake I in Enez		
	Lake Sultanhankoy	–			
Suloglu		8,500	Tuzla lake II in Kesan		
	Buyukgerdelli	910			
Enez		10,500	Altinyazi dam lake in Uzunkopru		
	Lake Dalyan	–			
	Lake Gala	–			
Meric		15,400	Degirmenci dam lake in Uzunkopru		
	Serem	345			
	Akcadam	460			
	Kuplu	2700			

Table 3 (continued)

Settlements of sub-provinces under flood hazard vulnerability	Population of settlements (year 2011)	Main water bodies	Main river flood plains	Mounts or hills (meters)
		Suloglu dam lake in Suloglu		
Subasi	2000			
Kadidondurma	800	Kocadere dam lake in Kesan		
Umurca	350			
Nasuhbey	300	Cavuskoy dam lake in Enez		
Alibey	265			
Karayusuflu	350	Umurbey dam lake in Enez		
Hasirciarnavutkoy	510			
Rahmanca	290	Dokuzdere dam lake in Kesan		
Lalapasa	7300			
Hamzabeyli	225	Koruklu dam lake in Kesan		
		Mecidiye dam lake in Kesan		

equals to the number of all the correctly classified cells divided by the total number of cells in the imagery (Congalton 1991; Congalton and Green 1999; Lillesand and Kiefer 2004, Jensen 2005; IDRISI 2013).

Conclusions

In conclusion, identification of the differential vulnerabilities of the entire Edirne flood risk areas to future flood hazards caused by global climate change is urgently required if measures are to be taken in time. To this end, the objective of this study was to contribute to future environmental planning and efficient flood management using a determined methodology to obtain geo-information effectively by analyzing landforms of the study region and to determine the flood hazard risk areas with their LULC types. In addition, a DTM of the study region was generated and interpreted to quantitatively and visually analyze the classification of the landforms. Additionally, the stream drainages were extracted and interpreted to obtain geo-information about the study region. The susceptible river flood plains due to heavy rainfalls and the flood risk areas of the settlements and agricultural areas in the study region were determined by analysis of both the DTM and the stream drainages. Determined landforms and stream drainages are substantially useful for interpreting the river flood risk areas and beneficial for decision-making on environmental planning in the future.

The accuracy of the study greatly relies on the resolution of the grid sizes of the DEM data and imagery, processing errors, quality of measurements, registration, transformation, and map projection. The approach would produce more detailed and accurate results if higher-resolution elevation data (e.g., LiDAR) and image data (e.g., GeoEye) were employed, particularly 5–10 m resolution. Nevertheless, the results with these data accuracies were promising for determining the flood risk areas of the settlements and agricultural areas.

Acknowledgments The financial support from the Izmir Institute of Technology is gratefully acknowledged.

References

ArcGIS (2013) Arc GIS 10.2 manual. Redland: ESRI. Available from http://www.esri.com

ASTER GDEM (2013) The Advanced Space-borne Thermal Emission and Reflection Radiometer, Global Digital Elevation Model data. Available from http://gdem.ersdac.jspacesystems.or.jp/

Atalay I (2008) Geography of regions in Turkey (in Turkish). Inkilap Press, Ankara

Band LE (1986) Topographic partition of watersheds with digital elevation models. Water Res 22(1):l5–l24

Baykan AR (2004) River basins in the environmental atlas of Turkey (in Turkish). Available from http://www.cedgm.gov.tr/CED/Files/cevreatlas%C4%B1/atlas_metni.pdf

Brivio PA, Colombo R, Maggi M, Tomasoni R (2002) Integration of remote sensing data and GIS for accurate mapping of flooded areas. Int J Remote Sens 23(3):429–441

Congalton RG (1991) A review of assessing the accuracy of classifications of remotely sensed data. Remote Sens Environ 37:35–46

Congalton RG, Green K (1999) Assessing the accuracy of remotely sensed data: principles and practices. Lewis, CRC, New York

Edirne Governorship, Turkey (2013) Available from http://www.Edirne.gov.tr/

El Sheimy N, Valeo C, Habib A (2005) Digital terrain modeling: acquisition, manipulation and applications. Artech House, Boston

ERSDAC (2013) ASTER Global DEM version 2 validation summary report at Earth Remote Sensing Data Analysis Center. Available from http://www.jspacesystems.or.jp/ersdac/GDEM/ver2Validation/Summary_GDEM2_validation_report_final.pdf

GLCF (2013) The Global Land Cover Facility: Earth Science Data Interface. Available from http://glcfapp.glcf.umd.edu:8080/esdi/

GEODATA (2013) Ministry of Forest and Water, GEODATA (Turkish: Orman ve Su Bakanligi). Available from http://geodata.ormansu.gov.tr/3d/indexv5.aspx

HGK (2013) General command of mapping (Turkish: Harita Genel Komutanligi). Available from http://www.hgk.msb.gov.tr/english/index.php

Ho LTK, Umitsu M, Yamaguchi Y (2010) Flood hazard mapping by satellite mimages and SRTM DEM in the Vu Gia–Thu Bon alluvial plain, Central Vietnam. International archives on the photogrammetry, remote sensing and space information science, volume XXXVIII, part 8, 275–280, Kyoto, Japan

Hoque R, Nakayama D, Matsuyama H, Matsumoto J (2011) Flood monitoring, mapping and assessing capabilities using RADARSAT remote sensing, GIS and ground data for Bangladesh. Nat Hazards 57:525–548

IDRISI (2013) Idrisi Selva 16.03 manual. Worcester: Clark labs, Clark University. Available from http://www.clarklabs.org/

Jensen JR (2005) Introductory digital image processing: a remote sensing perspective, 2nd edn. Prentice-Hall, Englewood Cliffs

Kandilioti G, Makropoulos C (2012) Preliminary flood risk assessment: the case of Athens. Nat Hazards 61:441–468

Kim J, Kuwahara Y, Kumar M (2011) A DEM-based evaluation of potential flood risk to enhance decision suppoprt system for safe evacuation. Nat Hazards 59:1561–1572

Lillesand TM, Kiefer RW (2004) Remote sensing and image interpretation. Wiley, New York

Mark DM, Dozier J, Frew J (1984) Automated basin delineation from digital elevation data. Geo-Processing 2:299–311

Meyer V, Scheuer S, Haase D (2009) A multi-criteria approach for flood risk mapping exemplified at the Mulde river, Germany. Nat Hazards 48:17–39

MGM (2013) Turkish state meteorological service–natural flood disaster (Turkish: Meteoroloji Genel Mudurlugu). Available from http://www.mgm.gov.tr/arastirma/dogal-afetler.aspx?s=taskinlar

O'Callaghan JF, Mark DM (1984) The extraction of drainage networks from digital elevation data. Computer Vision Graph Image Processing 28:328–344

Ozdemir H, Bird D (2009) Evaluation of morphometric parameters of drainage networks derived from topographic maps and DEM in point of floods. Environ Geol 56:1405–1415

San BT, Suzen ML (2005) Digital elevation model (DEM) generation and accuracy assessment from ASTER stereo data. Int J Remote Sens 26(22):5013–5027

Sanyal J, Lu XX (2004) Application of remote sensing in flood management with special reference to monsoon Asia: a review. Nat Hazards 33:283–301

Schanze J, Zeman E, Marsalek J (eds) (2006) Flood risk management: hazards, vulnerability and mitigation measures, Proceedings of the NATO advanced research workshop on flood risk management, vol 67. Czech Republic, Ostrov

TUIK (2013) Turkish Statistical Institute (Turkish: Turkiye Istatistik Kurumu). Available from http://www.turkstat.gov.tr

Van der Sande CJ, de Jong SM, de Roo APJ (2003) A segmentation and classification approach of IKONOS-2 imagery for land cover mapping to assist flood risk and flood damage assessment. International Journal of Applied Earth Observation and Geoinformation 4(3):217–229

Wang Y, Colby JD, Mulcahy KA (2002) An efficient method for mapping flood extent in a coastal floodplain using Landsat TM and DEM data. Int J Remote Sens 23(18):3681–3696

Wilson JP, Gallant JC (2000) Terrain analysis: principles and applications. Wiley, New York